



# Bis propargyl ether resins: synthesis and structure–thermal property correlations

C.P. Reghunadhan Nair\*, R.L. Bindu, K. Krishnan, K.N. Ninan

*Propellant and Special Chemicals Group, Vikram Sarabhai Space Centre, Trivandrum 695022, India*

Received 23 December 1997; accepted 4 February 1998

## Abstract

Bis propargyl ethers of bisphenol-A, (BPA), bisphenol ketone (BPK) and bisphenol sulfone (BPS) were synthesised and characterised. These monomers were thermally polymerised to the corresponding poly (bischromenes). The cure behaviour, as monitored by differential scanning calorimetry, depended on the structure of the monomer. The non isothermal kinetic analysis of the cure reaction using four integral methods revealed that the presence of electron-withdrawing group did not favour the cyclisation reaction leading to formation of chromene, which precedes the polymerisation and this is in conformation to the proposed mechanism of polymerisation. Thus, the cure temperature and activation energy for the reaction increased in the order BPA < BPK < BPS. The cure profile under isothermal and nonisothermal conditions could be simulated from the kinetic parameters. The substituent group bridging the two phenyl rings also influenced the thermal stability of the resultant polymers. Thus, sulfone and ketone-containing polymers were stabler than the isopropylidene-containing one. Kinetic analysis of thermal decomposition of the major step involving the chromene moieties revealed a two-stage degradation mechanism. The computed activation energies implied that the initiation of the degradation reaction was disfavoured by the electron-withdrawing nature of the bridge unit, probably through destabilisation of the intermediate radical. © 1998 Elsevier Science Ltd. All rights reserved.

## 1. Introduction

Acetylene-terminated monomers and polymers are gaining importance in view of the increased need for easily processible thermally stable polymers [1, 2]. Such polymers with a properly designed backbone could potentially serve as matrices in carbon-carbon composites [3] and in various high-performance polymer composite structures for space applications [4]. One key feature of these systems is their ability to undergo curing through addition reaction of the acetylene groups, either linearly or in cyclic way. The mechanism of polymerisation of the acetylene groups can be tuned by proper catalysis [5, 6]. For conferring thermal stability, cyclotrimerisation is preferred to linear polymerisation. In contrast to terminal acetylene or phenyl acetylene functional monomers, propargyl ether

derivatives are attractive from the point of view of ease of synthesis and polymerisation. Some studies have recently been devoted to the synthesis and polymerisation of a few propargyl ether systems [7–10]. However, most of the studies relate to understanding the mechanism of curing using model compounds. This paper concerns the synthesis of three structurally different bispropargyl ether monomers and their polymers. The influence of the structure on the cure behaviour of the monomers and on the thermal stability of the polymer has been examined. A detailed report on the kinetics of cure reaction and thermal decomposition has also been presented.

## 2. Experimental

### 2.0.1. Materials

Bisphenol-A (BA, 2,2-bis-[4-hydroxy phenyl] propane, SD Fine chemical, Mumbai, India), bisphenol

\* Corresponding author.

ketone (BK, 4,4'-dihydroxy benzophenone, Lancaster, UK), bisphenol sulfone (BS, bis[4-hydroxy phenyl] sulfone, Merck, Germany), propargyl bromide (1-bromo propyne, Merck, Germany) were used as received. All solvents were distilled prior to use.

#### 2.0.2. Instruments

IR was taken with a Nicolet FTIR model 510P.  $^{13}\text{C}$  NMR was taken on a Bruker-300 MHz spectrometer. Differential thermal analysis was carried out with a Mettler thermal analyser 3000 coupled to a DSC-20. Thermogravimetric analysis was carried out in nitrogen atmosphere on a Dupont TA-2000 connected to a 951 thermogravimetric analyser.

#### 2.0.3. Syntheses of bis propargyl ethers, BPA, BPK, BPS

In a typical synthesis, bisphenol-A (22.3 g, 0.1 mol) was dissolved in 100 ml freshly distilled dimethyl formamide, to which a solution of 8 g (0.2 mol) sodium hydroxide in 20 ml distilled water was added. To this, a solution of propargyl bromide (26.6 g, 0.22 mol) in 25 ml dimethyl formamide was added dropwise under agitation at room temperature. The reaction system was kept agitated at 70°C for 8 h. The product was

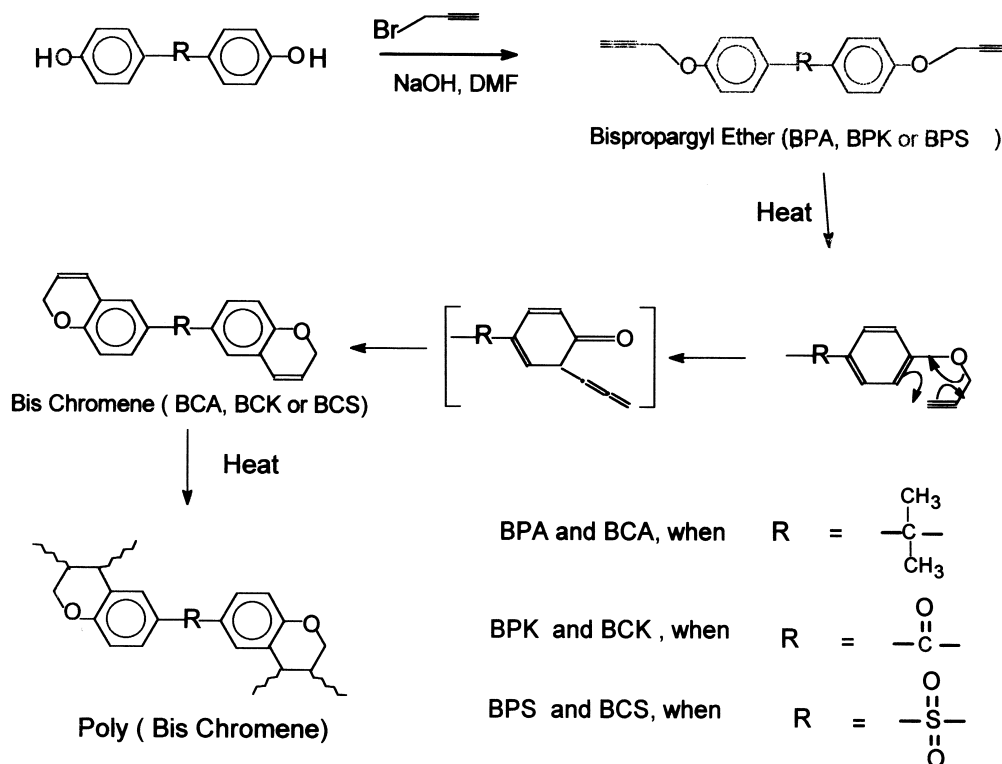
isolated by precipitating the mixture into 1 l of cold water. The product was filtered and dried at 50°C under vacuum. It was recrystallised from methanol to obtain the pale-yellow crystalline monomer in 80% yield. The other two monomers, BPK and BPS, were synthesised similarly. They were recrystallised from tetrahydrofuran–methanol mixture and were further purified by passing their solution through basic alumina column. Characterisation was carried out by spectral analyses (FTIR,  $^{13}\text{C}$  NMR).

#### 2.0.4. Polymerisation

The polymerisation was carried out by heating the monomers in vacuum at 260°C for 2 h. The polymer was characterised by FTIR.

### 3. Results and discussion

The reaction scheme for synthesis of the three monomers is shown in Scheme 1. The monomers were characterised by FTIR which showed the characteristic absorption owing to  $\equiv\text{C}-\text{H}$  bond of the propargyl groups at  $3272\text{ cm}^{-1}$ . The absorption owing to the  $\text{C}\equiv\text{C}$  appeared as a weak band at  $2225\text{ cm}^{-1}$ . The OH



Scheme 1. Synthesis of bis propargyl ethers and mechanism of their polymerization.

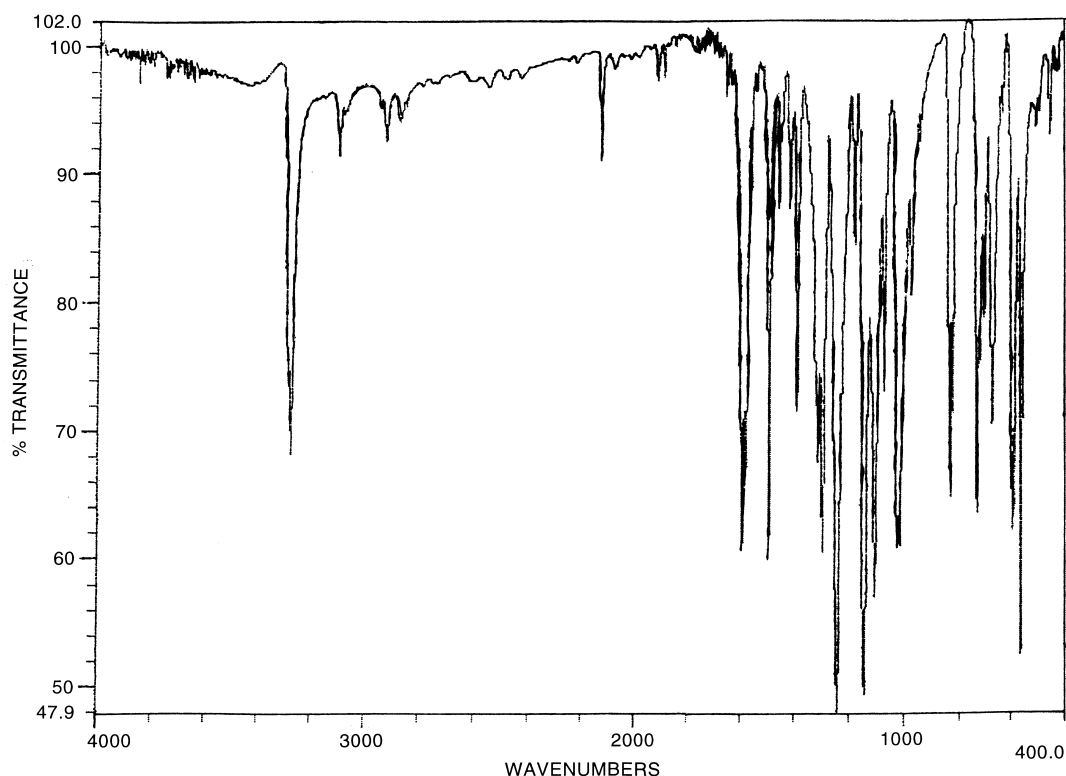


Fig. 1. FTIR spectrum of BPS.

peak of the precursor phenol was absent. BPK showed further absorption at  $1645\text{ cm}^{-1}$  owing to  $\text{C}=\text{O}$  group and the strong peaks owing to sulfone groups in BPS appeared at  $1150$  and  $1380\text{ cm}^{-1}$ . Typical IR spectrum of BPS is shown in Fig. 1.  $^{13}\text{C}$  analysis further confirmed the formation of the expected bispropargyl ethers. The  $^{13}\text{C}$  NMR spectra in the case of BPK and BPS are given in Fig. 2. The  $^{13}\text{C}$  NMR of BPA matched with the earlier reported spectrum for this compound [7].

Phenyl propargyl ethers are known to undergo Claisen type sigmatropic rearrangement to 2H-chromenes (2-H-1-benzopyrans) [11–13]. The uncatalysed rearrangement, in bulk is normally effected at higher temperature and is nearly always accompanied by thermal polymerisation of the formed chromene. Depending on the catalyst and conditions, rearrangement carried out in solution gives rise to a mixture of chromene and its polymer and some amount of methyl benzofuran as a secondary product. Thus, bispropargyl ethers on uncatalysed thermal polymerisation in bulk gives cross-linked bischromenes. The mechanism of polymerisation, shown in Scheme 1, has been well established through recent studies [10]. In the presence of certain specific catalysts, the propargyl group can undergo polymerisation through cyclotrimerisation of

the acetylene function [7]. In the present case, the above propargyl ethers on heating provided insoluble cross-linked polymers. FTIR confirmed the complete conversion of acetylene groups in the polymer.

### 3.1. DSC analysis

The cure characterisation of the monomers was carried out by DSC analysis. The DSC thermograms are shown in Fig. 3. All monomers show melting transition which increased with increasing polarity of the molecule. The cure reaction occurs at temperatures above  $200^\circ\text{C}$  and the cure profile depends on the monomer. The details of melting point and the cure temperature are given in Table 1 ( $T_{\text{ini}}$ =temperature of cure initiation;  $T_{\text{max}}$ =maximum in the exotherm;  $T_{\text{end}}$ =end of cure reaction). The exotherm is attributed to the Claisen rearrangement and the polymerisation. When mixed with  $\text{AgBF}_4$ , a catalyst known to facilitate Claisen rearrangement [12], another exotherm appeared at a lower temperature in the DSC, which is attributed to the catalysed rearrangement reaction. The exotherm at higher temperature is caused by the polymerisation of the rearranged product and the curing

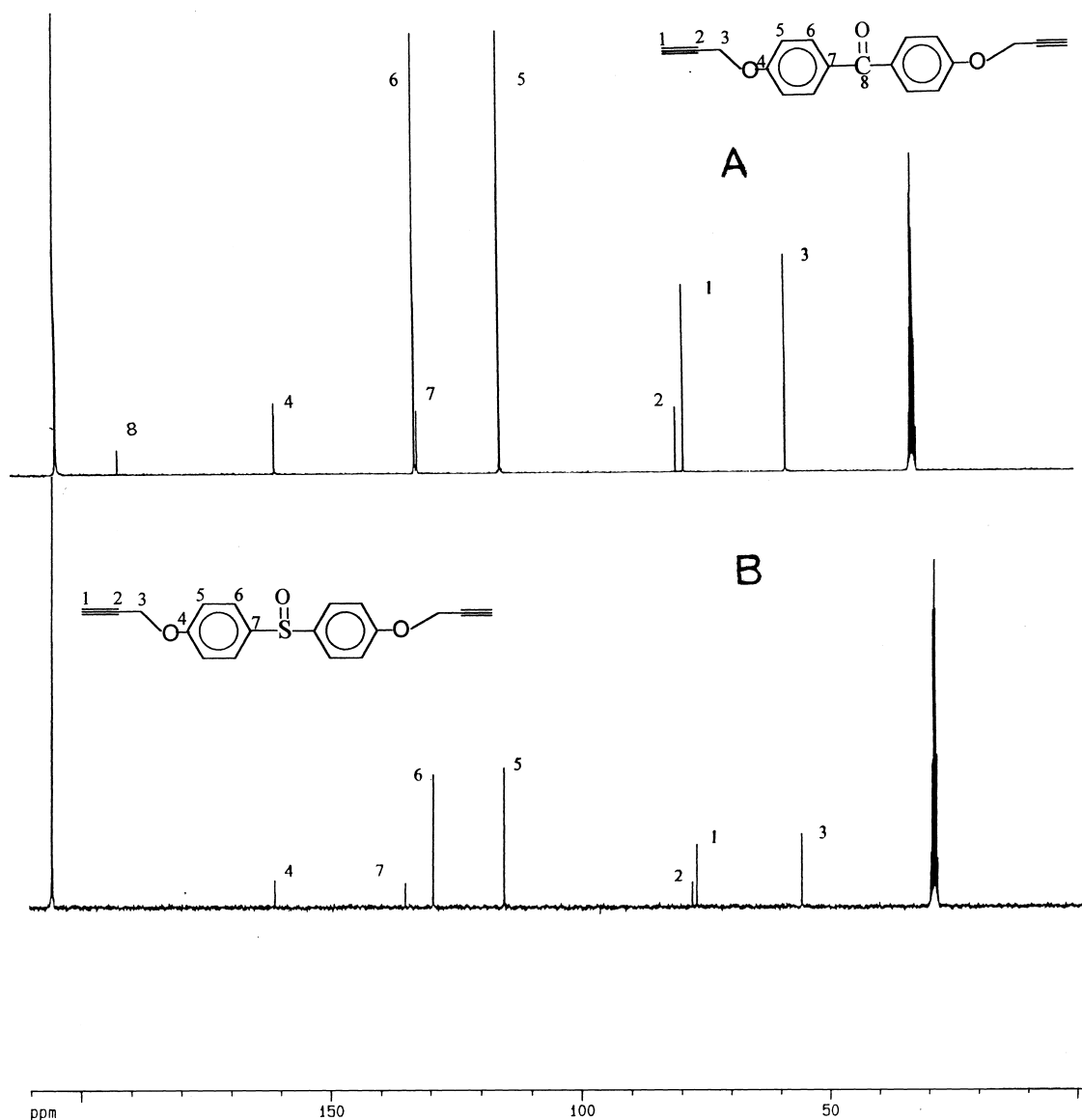


Fig. 2.  $^{13}\text{C}$  NMR spectra of A-BPK and B-BPS. Solvent  $d_6$ -acetone.

of any unrearranged monomer. On heating the catalysed system separately at the temperature corresponding to the first exotherm, some insoluble polymer was also found. This implies that the rearrangement at lower temperature is also accompanied by the polymerisation to some extent. For the uncatalysed system, the exotherm is observed at appreciably higher temperatures. This means that the rearrangement is immediately followed by polymerisation in the

uncatalysed system at high temperature. In this case, the rearrangement reaction can be considered as the rate determining step. Although the exotherm is caused by both the rearrangement reaction and the polymerisation, the DSC profile is determined by the kinetics of the former, which is the slow process. Since polymerisation immediately follows the rearrangement, the kinetics of the former can be expected to be in tune with that of the latter reaction and can be studied indirectly

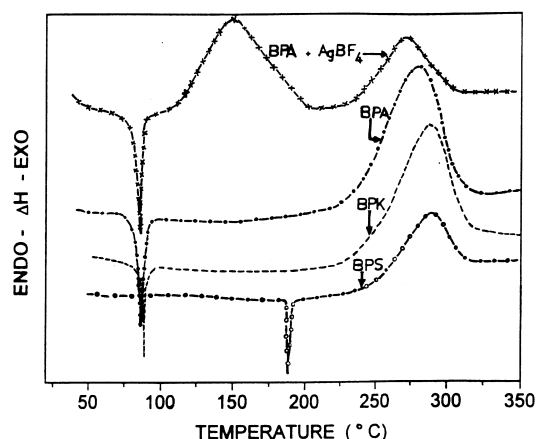
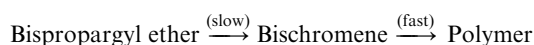


Fig. 3. DSC thermograms of BPA, BPK, BPS and BPA/AgBF<sub>4</sub> system. Heating rate = 10°C min<sup>-1</sup>.

from the DSC thermogram. The sequence of the reactions can be depicted as follows:



### 3.2. Kinetics of cure reaction

In non isothermal reaction, the rate expression can be given as

$$d\alpha/dT = (A/\phi)e^{-E/RT}(1-\alpha)^n \quad (1)$$

where  $\alpha$  is the fractional conversion at temperature  $T$ , following a heating rate  $\phi$ .  $E$  is the activation energy and  $A$  the Arrhenius frequency factor. The reaction order is  $n$ .

Several authors have integrated the above equation using different approximations, the noted ones among them are:

1. Coats–Redfern equation [14]

$$\ln\{g(\alpha)/T^2\} = \ln\{AR/\phi E(1-2RT/E)\} - E/RT$$

2. MacCallum–Tanner equation [15]

$$\log g(\alpha) = \log(AE/\phi R) - 0.483E^{0.435} - (0.449 + 0.217E) \times 10^3/T \quad (E \text{ in kcal mol}^{-1})$$

3. Horowitz–Metzger equation [16]

$$\ln g(\alpha) = \ln(ART_s^2/\phi E) - E/RT_s + E\theta/RT_s^2$$

4. Madhusudhanan–Krishnan–Ninan equation [17]

$$\ln\{g(\alpha)/T^{1.9215}\} = \ln(AE/\phi R) + 3.7721 - 1.9215 \ln E - 0.12039E/T$$

where  $g(\alpha) = \{1 - (1 - \alpha)^{1-n}\}/(1-n)$ ; for  $n \neq 1$ ,

Table 1  
Cure characteristics and related kinetic parameters of bispropargyl ether monomers

System	M.P. (°C)	T <sub>ini</sub> (°C)	T <sub>max</sub> (°C)	T <sub>end</sub> (°C)	n	Kinetic parameters					
						C-R	M-T	H-M	M-K-N		
						E (kJ/mol)	A (s <sup>-1</sup> )	E (kJ/mol)	A (s <sup>-1</sup> )	E (kJ/mol)	A (s <sup>-1</sup> )
BPA	81	189.6	285	318	0.7	152.9	1.90 × 10 <sup>12</sup>	154.6	2.63 × 10 <sup>12</sup>	168.5	6.02 × 10 <sup>13</sup>
BPK	87	196.3	289	334	1.0	169.6	6.31 × 10 <sup>13</sup>	171.3	8.71 × 10 <sup>13</sup>	190.9	6.60 × 10 <sup>15</sup>
BPS	189	221	289.6	315	1.0	211.3	5.75 × 10 <sup>15</sup>	213.4	8.91 × 10 <sup>15</sup>	233.2	6.76 × 10 <sup>19</sup>
										211.5	6.16 × 10 <sup>15</sup>

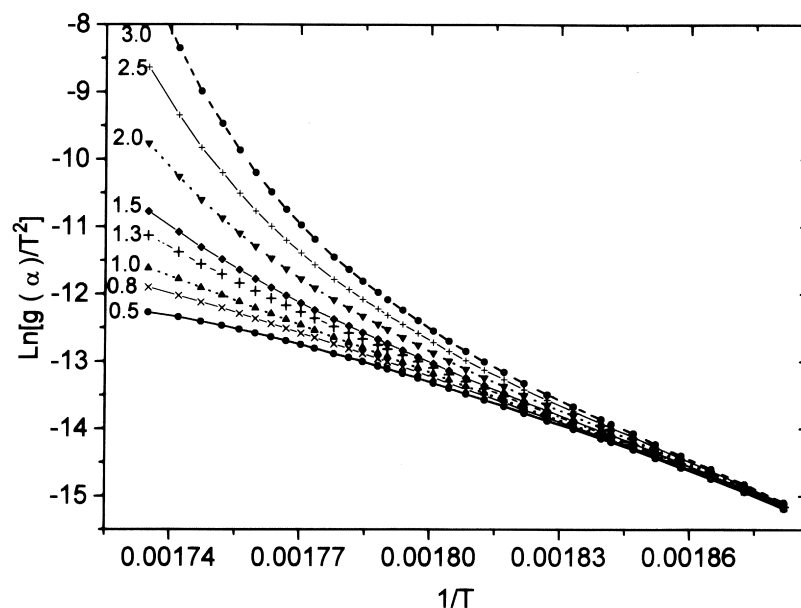


Fig. 4. Determination of reaction order by Coats-Redfern method for BPS.

$g(\alpha) = -\ln(1 - \alpha)$ .  $R$  is the gas constant.  $T_s$  corresponds to the peak temperature in differential thermogram and  $\theta = T - T_s$ .

The kinetic constants were calculated using the above equations.  $\alpha$  was estimated from the fractional enthalpy of reaction. Kinetic plots assuming different order of reaction were made using the C-R equation

and the best fit furnished the value of  $n$ . One such plot is shown in Fig. 4. The kinetic plots for determining  $E$  and  $A$  using the different equations for the optimised  $n$  are shown in Figs. 5–8. The kinetic constants for the three monomers are given in Table 1. The different methods give nearly consistent values (except in the case of the H-M method which gives slightly higher

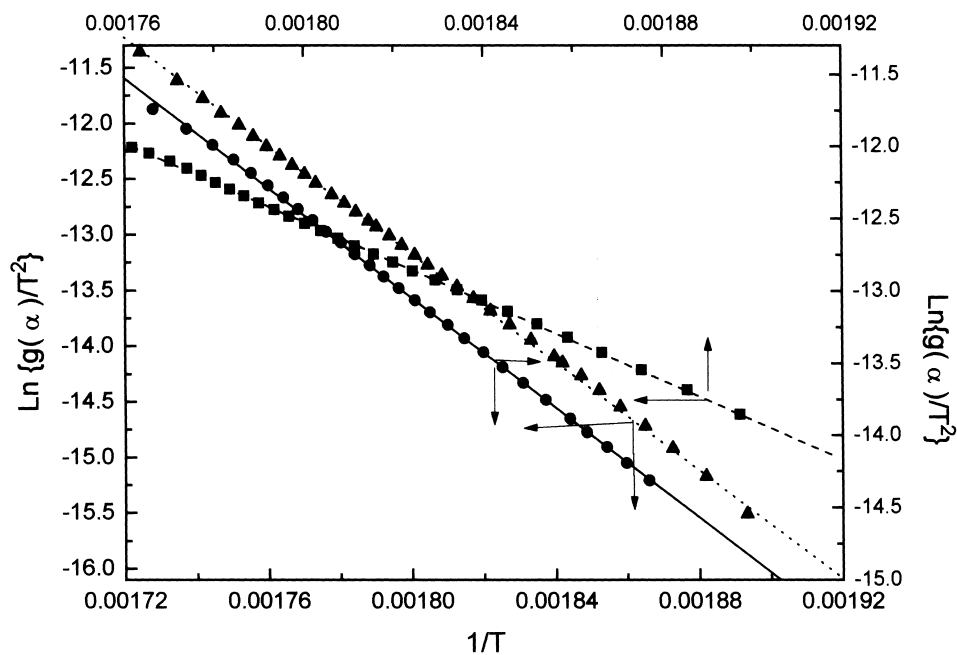


Fig. 5. Determination of kinetic parameters for cure reaction by C-R method = ■—BPA; ●—BPK, ▲—BPS.

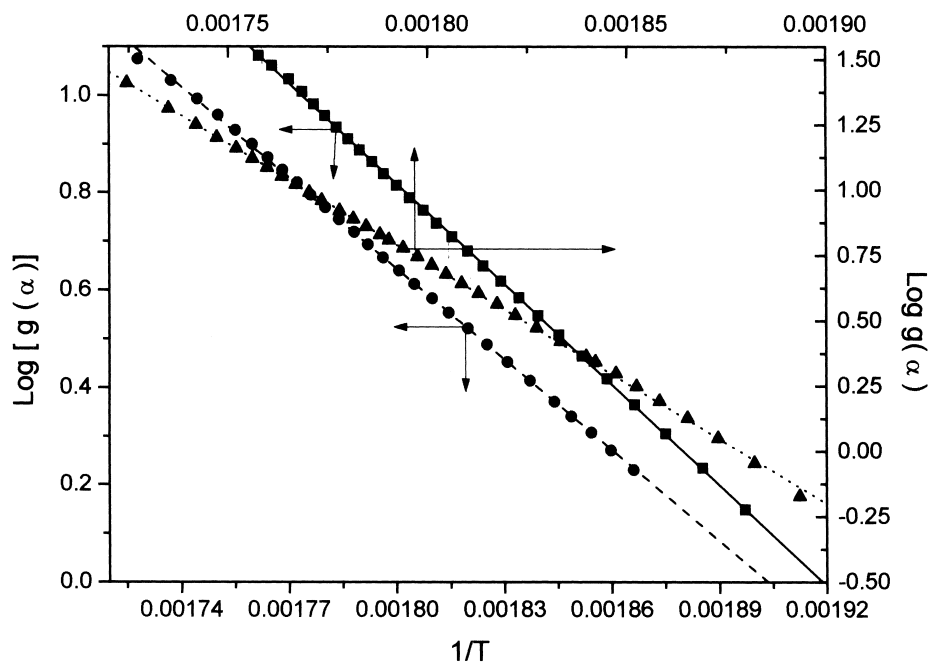


Fig. 6. Determination of kinetic parameters for cure reaction by M-T method = ■—BPA, ●—BPK, ▲—BPS.

values attributed to the approximation used in deriving this equation [18]. It may be noted that the cure reaction follows mostly first order. The activation energy is in the range 150–220 kJ/mol, depending on the structure, and is found to increase in the order

BPA < BPK < BPS. Interestingly, this order follows the order for the ease of the cyclisation reaction for formation of the chromene. The Claisen rearrangement, being electrophilic in nature, is retarded by the presence of electron-withdrawing groups on the ben-

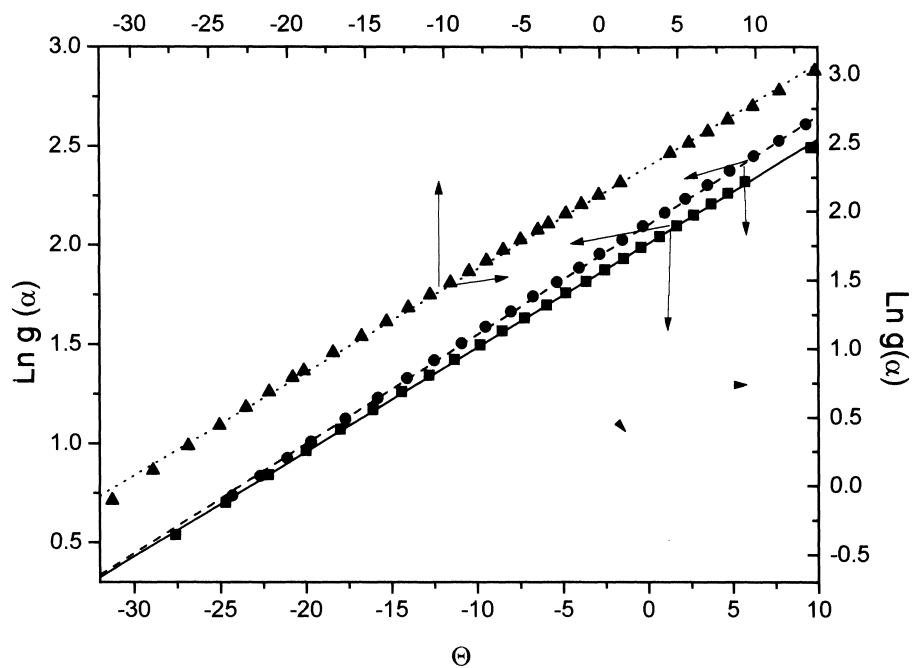


Fig. 7. Determination of kinetic parameters for cure reaction by H-M method = ■—BPA, ●—BPK, ▲—BPS.

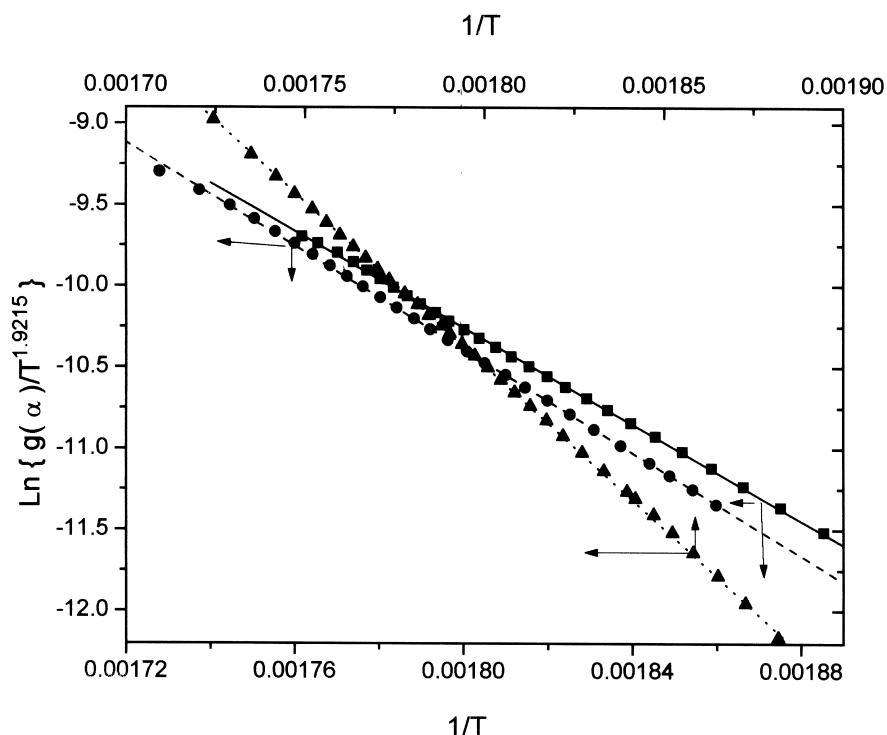


Fig. 8. Determination of kinetic parameters for cure reaction by M-K-N method = ■—BPA, ●—BPK, ▲—BPS.

zene ring. In the present case, sulfone group is more electron-withdrawing than the ketone group (in BPK), which in turn, is more electron-withdrawing than the isopropylidene group (in BPA). The computed activation energy follows this trend of the electron-withdrawing ability of the bridge substituent. A similar substituent effect has been reported for Claisen rearrangement of allyl phenyl ethers [19].

### 3.2.1. Isothermal studies

From the kinetic data obtained from the dynamic DSC, it is possible to predict the cure behaviour under isothermal conditions. The equation relating time, temperature and fractional conversion is given as,

$$\alpha = 1 - \{1 - A(1 - n)te^{-E/RT}\}^{1/1-n} \quad (2)$$

The time-conversion profiles, predicted for the isothermal cure of BPA at various temperatures using Eq. (2) are given in Fig. 9 along with the experimental results at 230°C. The experimental time-conversion plot at 230°C deviated from the predicted one at this temperature and was closer to the one at 245°C. The difference can be attributed to the thermal lag in dynamic experiment, which is more pronounced in materials of low thermal conductivity, as in the present system. Since the difference is dependent on the heating rate, reliable prediction requires establishment of the heating rate dependency on the difference in cure kinetics which is

not the main objective of the present study. The isothermal DSC data at 230°C for BPA were separately analysed by the conventional method using the kinetic expression,

$$d\alpha/dt = k(1 - \alpha)^n,$$

where  $k$  is the rate constant.

Rearranging,

$$\ln(d\alpha/dt) = \ln k + n \ln(1 - \alpha) \quad (3)$$

The linear plot according to Eq. (3) is shown in Fig. 10. The value of  $n$  was obtained as 0.73 which is very close to the value of 0.7 obtained from the dynamic data. The value of  $k$  works out to be  $7.58 \times 10^{-2} \text{ min}^{-1}$ , which is higher than the value calculated from the kinetic data from dynamic DSC analysis ( $= 1.5 \times 10^{-2} \text{ min}^{-1}$ ) for reasons stated above.

### 3.2.2. Simulation of DSC thermogram

From the kinetic data, it is possible to create back the DSC curves at different heating rates. In fact, the heat liberated at a given temperature is proportional to the fractional conversion at that temperature, which is related to rate of reaction by

$$dH/dT = (1/\phi)Ae^{-E/RT}(1 - \alpha)_T^n \quad (4)$$

In this case,  $\alpha$  at any temperature can be computed by accounting for the fractional conversion for the iso-



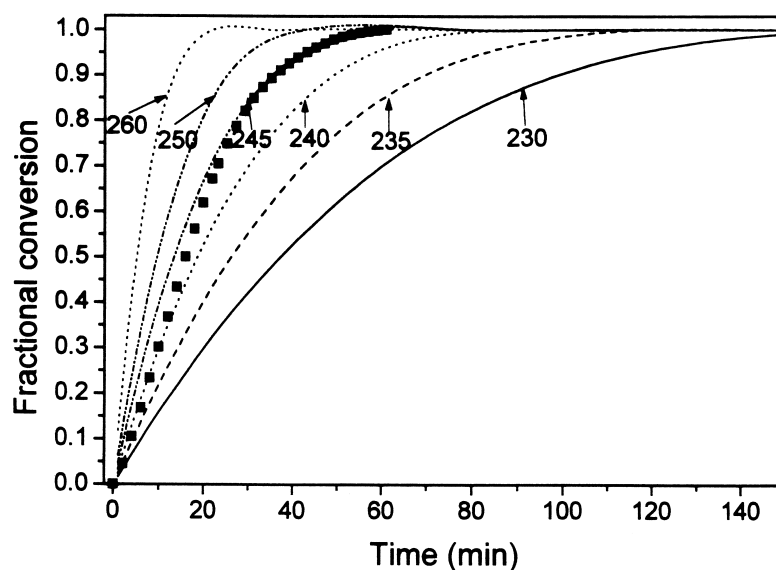


Fig. 9. Isothermal time-conversion profile prediction for BPA at various temperatures. ■—experimental data at 230°C.

thermal time increments of  $\Delta t$  at each temperature using Eq. (2) and adding until the required temperature.  $\Delta t$  can be taken as equal to  $1/\phi$ .

In fact,

$$(1 - \alpha)_T = \pi \Pi^T [1 - \{1 - A(1 - n) \Delta t e^{-E/RT}\}^{1/(1-n)}] \quad (5)$$

Using Eqs. (4) and (5), the DSC curve has been created for a typical case of BPA at different heating rates and is shown along with the normalised (for baseline) experimental DSC at a heating rate of 10°C

min<sup>-1</sup> in Fig. 11. A close match between the two shows the validity of the computed kinetic parameters.

### 3.3. Thermogravimetric analyses

The thermal stability of the cured poly (bis chromene)s, (poly (BCA), poly (BCK), and poly (BCS) correspondingly from BPA, BPK and BPS) was assessed by thermal analyses. The thermograms of the three polymers are compiled in Fig. 12. The polymers are

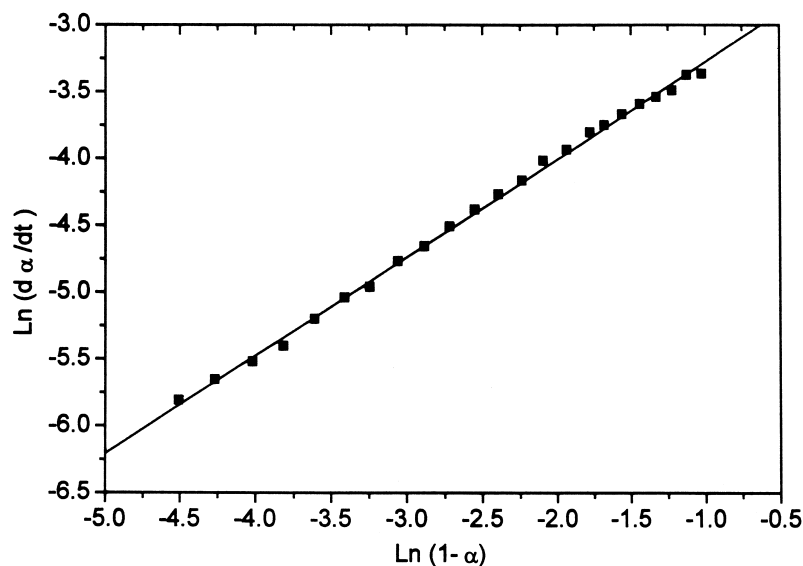


Fig. 10. Kinetic plot for determination of  $n$  and  $k$  from isothermal cure at 230°C for BPA.

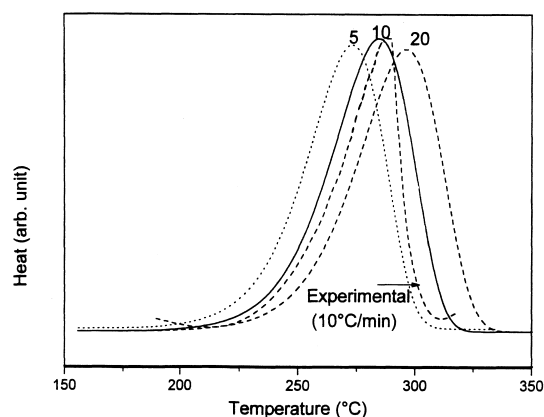


Fig. 11. Simulated DSC curves for BPA at different heating rates. ---- Experimental DSC curve at a heating rate of  $10^{\circ}\text{C min}^{-1}$ .

moderately thermally stable and the stability is dependent on the backbone structure. The thermal stability is better than that of epoxy resins and comparable with those of cyanate esters and PMR-type polyimides. Apparently, the thermal stability increases in the order poly (BCA) < poly (BCS) < poly (BCK). The bridging units play some role in determining the stability of the cured network. It may be noted that for poly (BCA), the decomposition proceeds in two stages. The first stage is initiated at the isopropylidene group, followed by the decomposition of the chromene moieties. For the other two systems, the bridge units are more stable and the decomposition is triggered at the comparatively weaker chromene groups at a relatively higher temperature. The pattern of decomposition triggered at these groups is also dependent on the backbone structure. The rate of degradation slows down as the bridge unit changes from isopropylidene to sulphone and to ketone. This shows that the electron-withdrawing character of the bridge unit is conducive for the stabilisation of the benzopyran (chromene) moiety. In all cases, the residue almost stabilises at around  $700^{\circ}\text{C}$  and, interestingly, the mass-loss at this

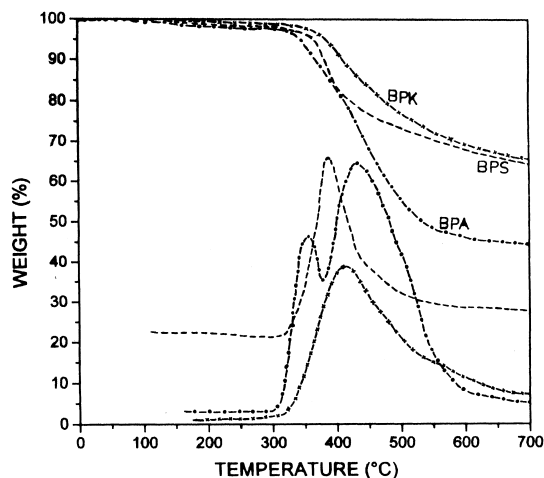


Fig. 12. Thermograms of polymers of BPA, BPK and BPS in  $N_2$ . Heating rate  $10^{\circ}\text{C min}^{-1}$ .

temperature corresponds to the percentage of fragile groups in the network. In calculating the latter, only the chromene moieties have been taken into account for poly (BCK) and poly (BCS), whereas for poly (BCA), this includes also the bridging isopropylidene groups. The thermal decomposition characteristics of the three polymers are compiled in Table 2 which also shows the good match between the experimental and calculated values for the mass-loss of fragile moieties.

The kinetics of decomposition of the major step involving the chromene moieties were analysed using the Coats–Redfern method. For calculating the fractional decomposition, the total mass-loss up to  $700^{\circ}\text{C}$  was considered for a comparison among the systems. In these cross-linked systems, the initiation can be expected to be random and, hence, the reaction can be assigned a first order. The kinetic analysis was limited to the major step involving the chromene moieties. A typical plot is shown in Fig. 13 which shows that this step consists of two thermal events. The first event can be ascribed to the initiation and the second to the continued decomposition and volatilisation that might fol-

Table 2  
Characteristics and kinetic parameters for the thermal decomposition of the cured polymers

Kinetic parameters (method, C–R)									
				Stage I		Stage II			
Polymer	$T_{\text{ini}}$ (°C)	Mass-loss at 700°C (wt%)	Fragile fragments, calculated (wt%)	$E$ (kJ/mol)	$A$ (s <sup>−1</sup> )	Mass-loss range (wt%)	$E$ (kJ/mol)	$A$ (s <sup>−1</sup> )	Mass-loss range (wt%)
PBCA	340	57	51	194.9	$7.71 \times 10^{11}$	83–72	68.0	$4.65 \times 10^2$	71–53
PBCK	370	36	38.6	95.5	$2.74 \times 10^4$	94–88	26.2	$5 \times 10^2$	87–80
PBCS	350	33	34.4	142.8	$5.74 \times 10^8$	96–86	51.2	$1.43 \times 10^1$	85–80

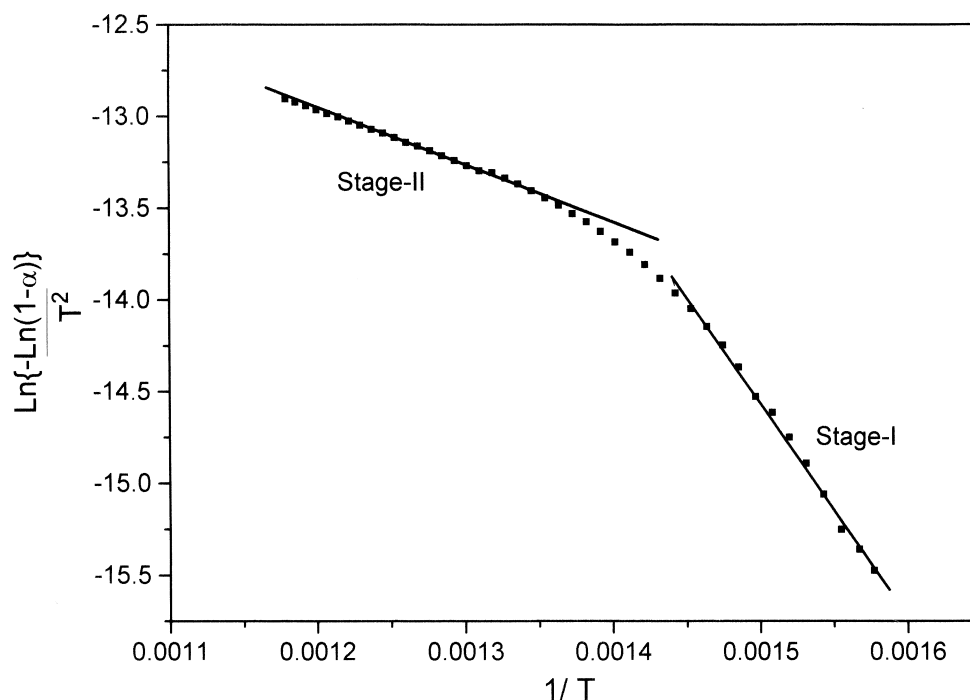
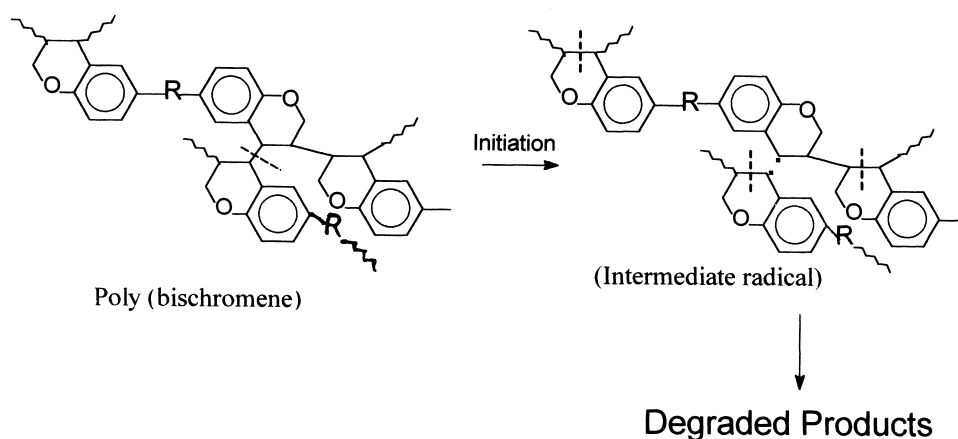


Fig. 13. Plot for determination of kinetic parameters for the thermal degradation of poly (BCK).

low a different mechanism. The activation energies for both stages depended on the bridge units, although the groups undergoing degradation were the same for all. The possible mechanism for initiation of thermal degradation of the crosslinked chromene is shown in Scheme 2. The decomposition must be triggered at the crowded carbon giving rise to benzyl-type free radicals whose stability is decreased by the presence of electron-withdrawing substituents on the phenyl ring. Consequently, the initiation is less facilitated for BPS

than for BPK and thus, the activation parameters are higher for BPS. Since the radicals in poly (BCS) are more unstable, they undergo rapid secondary reaction and as a result, the degradation proceeds faster for this case. The second stage for poly (BCS) also has a higher  $E$  than the corresponding stage for poly (BCK). For poly (BCA), however, the activation energies were the highest. This molecule, after the loss of isopropylidene groups in the initial stages, assumes a different structure bearing the chromene. Hence, a correct corre-



Scheme 2. Probable mechanism of degradation of poly(bischromenes).

lation with the structure could not be obtained. The low activation energy and frequency factor for the second stage imply that it is associated with volatilisation. The kinetic constants and the corresponding mass-loss ranges are given in Table 2.

#### 4. Conclusion

Bispropargyl ethers, based on three bisphenols, gave rise to bischromene network polymers on heating. The cure characteristics, as well as the thermal stability of the cured network, depended on the structure of the monomers. The electron-withdrawing nature of the bridge-substituent of the bisphenol disfavoured the rearrangement reaction preceding the polymerisation. The activation energy for the curing reaction showed a proportionate trend. The electron-withdrawing nature of the bridge groups also increased the activation energy for the initiation of thermal decomposition of chromene groups in the network.

#### Acknowledgements

The authors are grateful to their colleagues in the Analytical and Spectroscopy Division for support in analyses. The permission granted by the Director, VSSC to publish this paper is gratefully acknowledged. R.L.B. thanks CSIR, New Delhi for the award of a fellowship.

#### References

- [1] Lee CY-C, Pritchard G, editors. *Developments in reinforced plastics*. Barking: Elsevier, 1986;5:121–150.
- [2] Hergenrother PM, Mark HF, Bikales NM, Overberger CG, Menges G, Kroshwitz JJ, editors. *Encyclopaedia of polymer science and engineering*, 2nd ed. New York: Wiley, 1985;1:61–86.
- [3] Baklouti M, Chaagouni R, Fontanille M, Villenave J-J. *Eur. Polym. J.* 1995;31:215.
- [4] Katzman HA, Mallen JJ, Barrey WT. *J. Adv. Mater.* 1995;21:.
- [5] Douglas WE, Overend AS. *J. Mater. Chem.* 1994;4:1167.
- [6] Douglas WE, Overend AS. *Polym. Commun.* 1991;32:495.
- [7] Douglas WE, Overend AS. *Eur. Polym. J.* 1991;27:1279.
- [8] Douglas WE, Overend AS. *J. Mater. Chem.* 1993;3:27, 1019.
- [9] Douglas WE, Overend AS. *Polymer*, 1993;34:1544; *J. Org. Metall. Chem.* 1995;444:C-62.
- [10] Grenier-Loustalot MF, Sangler C. *Eur. Polym. J.* 1997;33:1125.
- [11] Zsindely J, Schmidt H. *Helvetica* 1968;51:1510; Pomeranz UK, Hansen H-J, Schmidt H. *Helvetica* 1973;56:2981.
- [12] Hug R, Frater Gy, Hansen H-J, Schmidt H. *Helvetica* 1971;54:306.
- [13] Rao U, Balasubrahmanian KK. *Tetrahed. Lett.* 1983;24:5023.
- [14] Coats AW, Redfern JP. *Nature* 1964;201:68.
- [15] MacCallum JR, Tanner J. *Eur. Polym. J.* 1970;6:1033.
- [16] Horowitz HH, Metzger G. *Anal. Chem.* 1963;35:1464.
- [17] Madhusudhanan PM, Krishnan K, Ninan KN. *Thermochim. Acta* 1986;97:189.
- [18] Nair CGR, Ninan KN. *Thermochim. Acta* 1978;23:161.
- [19] Goering HI, Jacobson RR. *J. Am. Chem. Soc.*, 1958;80:3277; White WN, Gwynn D, Schlitt R, Girard C, Fife WK. *J. Am. Chem. Soc.* 1958;80:3271; White WN, Slater CD. *J. Org. Chem.* 1962;27:2908.